Zbyszko Kazimierski
Professor.

Lech Brzeski
Assistant Professor.

Longin Horodko
Research Scientist.

Technical University of Lodz,
I-10, 90-924 Lodz, Poland

Gas Bearing of Infinite Stiffness

The experiences gathered during the theoretical and experimental investigations of the thrust and journal high stiffness bearing (H.S.B.) allowed to improvement of their characteristics. New elements of the throttling system were introduced into the journal H.S.B. to make possible this improvement. It was shown that the H.S.B. can reach infinite stiffness in a wide range of the loading forces having at the same time zero or submicronic shaft displacement. Additionally, the load-displacement characteristic of the H.S.B. may have the prescribed negative displacement to make possible the full compensation of elastic deformation of connected machine parts. The influence of journal rotation on the H.S.B. load-displacement characteristics is discussed in this paper. The H.S.B. of presented characteristics may be applied to many precise devices, e.g., to ultra-precision grinding machines.

1 Introduction

A new type of high stiffness journal and thrust bearings (H.S.B.) has been presented over 10 years ago by Brzeski and Kazimierski (1979), Kazimierski and Makowski (1981) and Brzeski et al. (1975–1979). These bearings differ from other constructions of the high stiffness bearings described by Tully (1976), Blondel et al. (1976), and Aoyama (1990). The load-displacement characteristics of the journal H.S.B. published by Brzeski and Kazimierski (1979) exhibited very high stiffness of the H.S.B. but in very narrow range of the loading force and had to be significantly improved.

The new elements of the journal H.S.B. throttling system have been introduced making possible the change of the load-displacement characteristics and to reaching very high stiffness in a wide range of the loading forces. These new elements are presented in the next part of this paper.

Two points of view on the H.S.B. characteristics are considered in this paper.

First, the infinite stiffness of the bearing itself.

Second, the entire compensation of mechanical deformations of the set consisted of the gas bearing and deformable connected parts of the machine.

In the second view, the load-displacement characteristics of the bearing have to exhibit the prescribed negative shaft displacements (opposite the loading force direction), which compensate the mechanical deformations of the connected machine parts.

The characteristics presented in this paper were obtained numerically basing on the computational model of the H.S.B., which was verified many times by comparisons with experiments.

The results discussed in this paper have been calculated for the aerostatic condition of the H.S.B. operation but the effects of high frequency journal rotation are considered and explained in Section 4.

Contributed by the Tribology Division for publication in the JOURNAL OF TRIBOLOGY. Manuscript received by the Tribology Division April 19, 1991; revised manuscript received October 20, 1991. Associate Technical Editor: D. C. Sun.

2 New Elements of Journal H.S.B. Construction

The principle of the journal H.S.B. operation is given in the paper by Brzeski and Kazimierski (1979) and will not be repeated in this paper.

The journal H.S.B. is presented in Fig. 1 and Fig. 2. The essential part of the bearing is movable bush 3 mounted by means of elastic rings 4 and elastic baffles 11 in the casing 6. The elastic rings 4 and baffles 11 play role of sealings only. They have the form of pneumatic tires pressurized by the supply pressure p_0. This solution has been tested successfully during the experimental investigations of the H.S.B. (Brzeski and Kazimierski, 1979; Kazimierski and Makowski, 1981). The drawing of such a sealing is shown inside the circle situated at the lower part of Fig. 1. It should be taken into account that $h_2 = 0(10^{-2})$ mm and $q_k \approx 10$ mm. The photo of the outer surface of the bush 3 has been presented in the paper by Brzeski and Kazimierski (1979), where the grooves of the depth g_k can be seen.

The throttling elements 10 are located between orifices 7 for feeding gas into chamber 1 and holes 8 for carrying of the gas from chamber 2 to the clearance existing between the shaft 9 and bush 3. The flow cross-section between the throttling elements and casing depends on the position of the bush relative to the casing and on the length of the throttling gap B, Fig. 2. The length $B = (2\pi/z - \gamma_c)R_2$ employed in the early investigations lead to unsatisfactory load-displacement characteristics (Brzeski and Kazimierski, 1979). Many experiences gathered during the H.S.B. investigations showed that the essential improvement of this characteristic may be achieved by reduction of the length B. This length may be limited by the additional circumferential elastic insertions 5, shown in Fig. 2, so that $B = (2\pi/z - \gamma_s) R_2$, where $\gamma_s > \gamma_c$. Technical realization of the idea of the length B changes may be different. A simple case of the succeeding changes of B has been introduced in the test rig described by Kazimierski and Makowski, 1981. The fluent variation of the length B is also possible, but requires a more complicated mechanical realization which will be the subject of further publications. The kind of this realization has no meaning for the computational mode used in this paper. The only important computational parameter is the throttling element cross-section $A_s = Bh_2$.

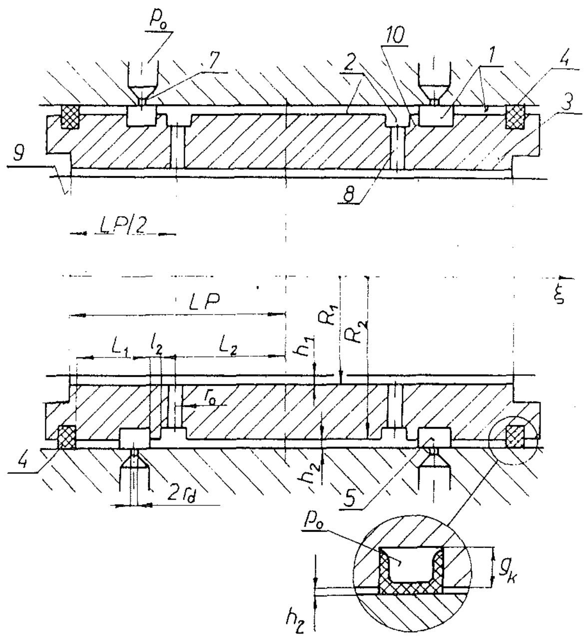

Fig. 1 Schematic diagram of the journal H.S.B., axial—section

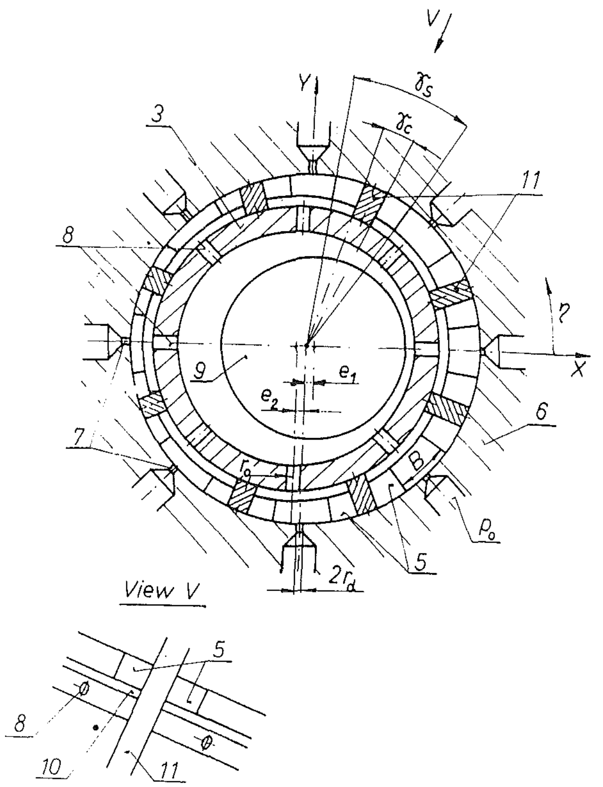

Fig. 2 Schematic diagram of the journal H.S.B., cross—section

3 Characteristics of Journal H.S.B.

An example of the journal H.S.B. of the main dimensions $R_1 = 55$, $L = 150$, $R_2 = 80$, $c_1 = 0.03$, $c_2 = 0.02$ (see Fig. 1 and 2, all dimensions in mm) and supply pressure $p_0 = 7$ bar is discussed in this part of the paper.

The H.S.B. feeding system produces pressure differences between loaded and unloaded sides of the shaft big enough to ensure satisfactory load capacity of the bearing.

It was checked numerically that the journal H.S.B. can always attain the loading capacity not less then the optimized ordinary bearing of the same main dimensions and supply pressure. For the considered case of bearing at $\epsilon_1 = 0.5$ the optimum carrying capacity is about 3000 N. ϵ_1—is the nondimensional relative eccentricity ratio between the shaft and movable bush. The loading forces shown in Figs. 4 and 5 reach the mentioned above load of the optimizea ordinary bearing.

The load-displacement characteristic of the journal H.S.B. published by Brzeski and Kazimierski (1979) exhibits very small displacements and locally very high stiffness but only for comparatively low loads F and in the region of negative absolute shaft displacements $e_1 < 0$. The improvement of the load-displacement characteristic shape was the main aim of the further investigations.

The journal H.S.B. reported in the above mentioned paper did not have the circumferential insertions 5 (Fig. 2), so that $\gamma_s = \gamma_c$, where γ_c is the angle which determines the width of the elastic buffles 11 (Fig. 2).

The change of the journal H.S.B. characteristic shape was attained by changing of the elastic insertions 5 length which lead to the variation of the throttling element length B (Fig. 2).

First, this solution has been introduced to the thrust H.S.B. and very attractive characteristics have been obtained. An unpublished example of such a characteristic is shown in Fig. 3.

The computational results of the journal H.S.B. characteristics with the changeable length of the throttling elements B are shown in Fig. 4 and Fig. 5.

The characteristics are calculated for the aerostatic conditions of the bearing operation.

The right-side part of Figs. 4 and 5 present the curves of

Nomenclature

B = length of the throttling element, Fig. 2
c_1, c_2 = mean values of radial clearance, shaf-bush, and bush-casing
e_1, e_2 = absolute displacements of shaft and bush, Fig. 2
e_{r1} = relative displacement of shaft with respect to bush
e_{1p} = projection of vector $\bar{e}_1$ on force line direction, Eq. (4)
F = loading force
$FB(=F/p_aR_1^2)$ = dimensionless force
g_k = depth of grooves, Fig. 1
h_1, h_2 = local film thicknesses, shaft-bush, and bush-casing
L_1, L_2 = dimensions shown in Fig. 1
LP = half of bearing length, Fig. 1
p_a, p_0 = atmospheric and supply pressures
R_1, R_2 = shaft radius and outer radius of bush, Fig. 1
r_0 = radius of plain feedhole, Fig. 1 and Fig. 2
r_d = radius of orifice, Fig. 1 and Fig. 2
z = number of baffles, Fig. 2
γ_c, γ_s = angles shown in Fig. 2
ϵ_1 = relative eccentricity ratio, shaft-bush
ϵ_2 = absolute eccentricity ratio, bush-casing

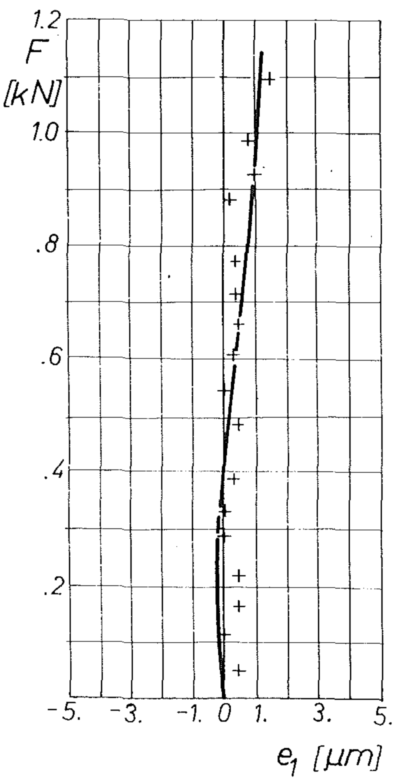

Fig. 3 Load-displacement characteristic of the thrust H.S.B. with varying B; — calculations, + + + + experiments

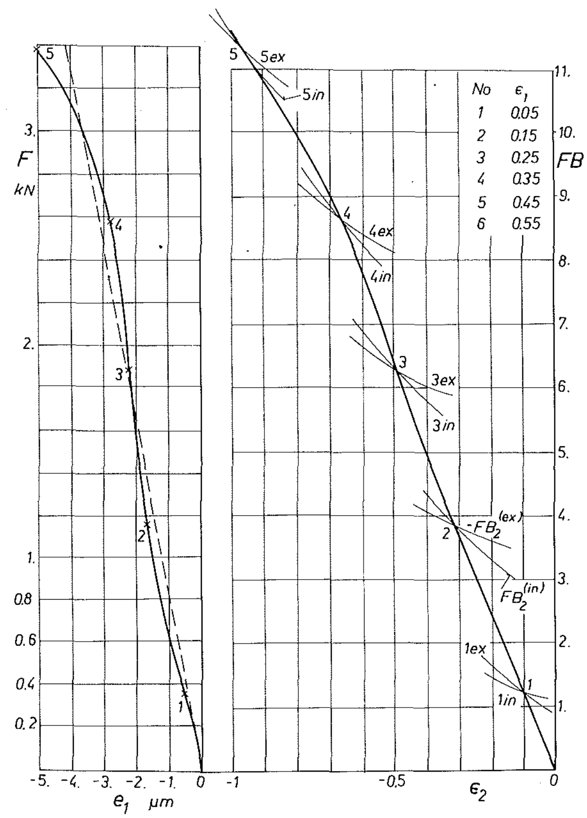

Fig. 5 The journal H.S.B. characteristic of a prescribed negative shaft displacement

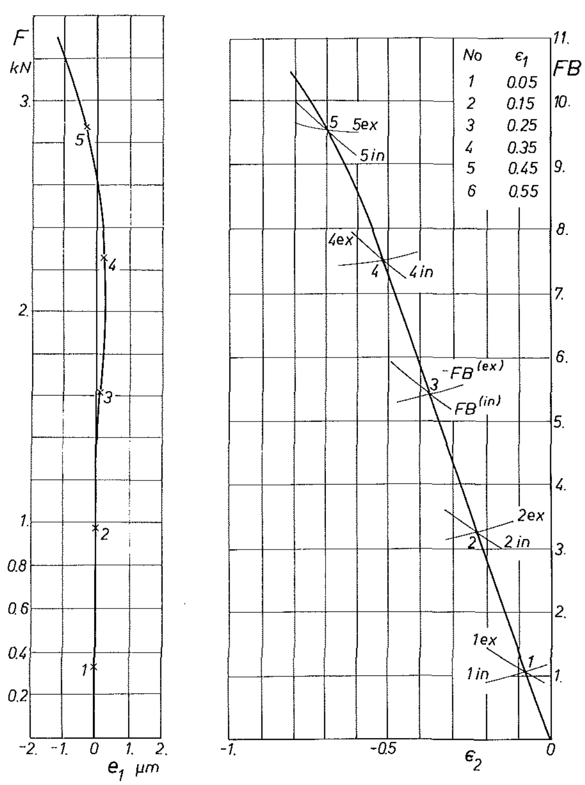

Fig. 4 The infinite stiffness journal H.S.B. characteristic

equilibrium between external $FB^{(ex)}$ and internal $FB^{(in)}$ nondimensional forces acting on cylindrical surfaces of the movable bush. The curves are plotted as functions of the bush eccentricity ϵ_2 for different values of the relative shaft eccentricities ϵ_1 marked in Figs. 4 and 5 by numbers 1–6. The absolute shaft displacement $e_1 = \epsilon_1 c_1 + \epsilon_2 c_2$ may be determined if the bush eccentricity of equilibrium ϵ_2 is read out from the equilibrium curves shown in Figs. 4 or 5. The loading forces F are presented in the left parts of Figs. 4 and 5 as functions of the absolute shaft displacements e_1.

A proper selection of the dimensions r_0, r_d, γ_s, L_1, and L_2 (see Fig. 1 and Fig. 2) makes it possible to obtain the characteristics shown in Fig. 4 and Fig. 5.

The absolute values of the shaft displacements plotted in Fig. 4 are equal to, zero in the range $0 \leq F < 1500$ N and for $1500 < F \leq 2800$ are less then 0.2 μm. This result shows that the H.S.B. constructed according to the presented principle may reach infinite or very high stiffness in a wide range of the loading forces having at the same time zero or submicronic shaft displacements.

One can consider another treatment of the stiffness problem then the stiffness of the bearing itself.

The entire compensation of the mechanical deformations of the set composed of a gas bearing and connected deformable parts of a machine may be taken into account. In this case the load-displacement characteristic has to exhibit the prescribed negative shaft displacement which compensates the deformations of the connected machine elements.

The example of such a characteristic is shown in Fig. 5.

The bearing of presented characteristic makes it possible to compensate the mechanical, deformations of connected parts illustrated in Fig. 5 by the dashed line. This line is a mirror reflection of the real positive stiffness characteristic of these elements (about 820 N/μm). The load-displacement bearing characteristic of the type shown in Fig. 5 has to be adjusted to the known stiffness diagram of the connected parts of the machine.

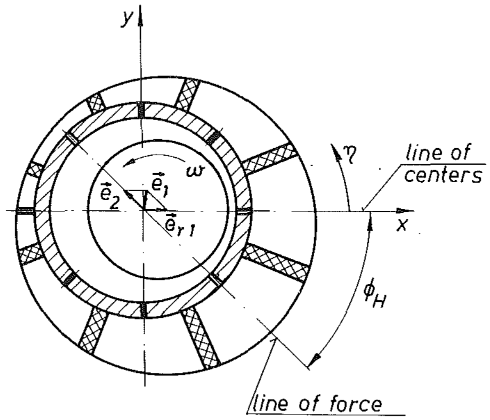

Fig 6 The effect of journal rotation of the H.S.B.

4 Effects of Hybrid H.S.B. Operation

Since the important applications of the H.S.B. are in the high speed grinding area, the effect of journal rotation must be taken into account.

According to the paper by Brzeski and Kazimierski (1979), the absolute shaft displacement e_1 was expressed as the following sum:

$$e_1 = \epsilon_1 c_1 + \epsilon_2 c_2 \qquad (1)$$

where: $\epsilon_1 c_1 = e_{r1}$ is the relative displacement of the shaft with respect to the movable bush, and

$\epsilon_2 c_2 = e_2$ is the absolute displacement of the bush with respect to the casing.

For the aerostatic conditions of the H.S.B. operations the displacements e_1, e_{r1}, and e_2 are measured along the x-axis.

Generally, the absolute shaft displacement may be presented as the following vector sum:

$$\mathbf{e}_1 = \mathbf{e}_{r1} + \mathbf{e}_2. \qquad (2)$$

If the aerostatic H.S.B. operation takes place the vectors $\mathbf{e}_{r1}$ and $\mathbf{e}_2$ act along the x-axis and they are directed opposite each other.

The full compensation (infinite stiffness) of the aerostatic H.S.B. is achieved if $e_1 = 0$, i.e.,

$$|\mathbf{e}_{r1}| = |\mathbf{e}_2| = e_s \qquad (3)$$

For hybrid operation of the H.S.B. when the shaft rotates the situation changes and vectors $\mathbf{e}_{r1}$ and $\mathbf{e}_2$ do not act along the same line. Figure 6 repeats the scheme of the H.S.B. construction shown in Fig. 2 with the rotating shaft. For this case we assume that $\mathbf{e}_{r1}$ is directed along the x-axis. The shaft rotation (with the angular velocity ω directed as it is shown in Fig. 6) causes that the loading force acts along the line inclined at some angle ϕ_H with respect to x-axis. The return movement of the bush is directed along the line of force as it is shown in Fig. 6.

Vector $\mathbf{e}_1$ may reach a significant value for hybrid operation of the H.S.B. if the aerostatic condition $|\mathbf{e}_{r1}| = |\mathbf{e}_2|$ is fulfield.

The stiffness of the hybrid H.S.B. is defined as $\dfrac{\partial F}{\partial e_{1p}}$, where e_{1p} is the projection of $\mathbf{e}_1$ on the force direction.

If the relation between $|\mathbf{e}_{1r}|$ and $|\mathbf{e}_2|$ is given by Eq. (3) e_{1p} for the hybrid H.S.B. is expressed by the formulae:

$$e_{1p} = |\mathbf{e}_1| \sin\frac{\phi_H}{2} = 2e_s sin^2\frac{\phi_H}{2}$$

$$\text{e.g., for } \phi_H = 25°;\ e_{1p} = 0.094 e_s. \qquad (4)$$

The above example shows, that the aerostatic condition, expressed by Eq. (3), may lead to the significant value of e_{1p} for hybrid operation of the H.S.B.

The most interesting infinite stiffness characteristic of the H.S.B. with rotating shaft is attained if $e_{1p} = 0$, in a wide range of the loading forces. The condition $e_{1p} = 0$ is fulfield if:

$$\mathbf{e}_1 \bullet \mathbf{e}_2 = 0 \qquad (5)$$

For the scheme of vectors shown in Fig. 6. Equation (5) leads to more general relation between $|\mathbf{e}_{r1}|$ and $|\mathbf{e}_2|$ than that expressed by Eq. (3), namely:

$$|\mathbf{e}_2| = |\mathbf{e}_{r1}| \bullet \cos\phi_H \qquad (6)$$

This relation should be taken into account during determination of the load-displacement characteristics of the hybrid H.S.B.

5 Conclusions

The proper selection of the geometrical parameters of the H.S.B. throttling system makes it possible to obtain the characteristic presented in Fig. 4. This result shows that the considered H.S.B. may reach the infinite stiffness in a wide range of the loading forces exhibiting at the same time zero or submicronic shaft displacements. Characteristic presented in Fig. 4 shows the infinite stiffness in the range $0 \leq F < 1500$ N at zero shaft displacements, and the stiffness about 2500 N/μm in the range $1500 < F \leq 2800$ N at shaft displacements less then 0.2 μm.

The next important results are shown in Fig. 5. The H.S.B. characteristic can be designed so that it exhibits a prescribed negative shaft displacements, which compensates deformations of connected machine elements.

It has been proved additionally that the H.S.B. attains always the loading capacity not less than the optimized ordinary bearing of the same main dimensions and supply pressure.

The analysis of the effect of journal rotation has been made and the condition which ensures the infinite stiffness of the hybrid H.S.B. is presented.

The journal and thrust H.S.B. of the described characteristics may be applied e.g., to ultra-precision grinding machines. The H.S.B. designed with a prescribed negative shaft displacements may be used for compensation of an elastic spindle and grinding fixture deformations. The H.S.B. characteristic can be then adjusted to the known stiffness diagram of the mentioned mechanical parts of the machine.

References

Aoyama, T., 1990, "Increase of Stiffness of Externally Pressurized Air Bearings with Automatic Controlled Restrictor," Raports No. 10, Research Group for Manufacturing Science, Keio University, Yokohama, p. 33.

Blondel, E., Snoyes, R., and Devrieze, L., 1976, "Externally Pressurized Bearings with Variable Gap Geometries," *Proc. of 7th Int. Gas Bearin Symp.*, Cambridge, England, Paper E2.

Brzeski, L., et al., 1975–1977, "Fluid Lubricated Bearing," Polish Patent P-167778, 1975; USA Patent No. 3960414, 1976; British Patent No. 1467911, 1977; USSR Patent No. 645614, 1979.

Brzeski, L., and Kazimierski, Z., 1979, "High Stiffness Bearing," ASME, Journal of Lubrication Technology, Vol. 110, pp. 520–525.

Kazimierski, Z., and Makowski, Z., 1981, "Investigations of High Stiffness Gas Lubricated Thrust Bearing," *Proc. of 8th Int. Gas Bearing Symp.*, Leicester, England, Paper 2.

Tully, N., 1976, "Static Performance and Stability of a Self Controlled Restrictor Gas Lubricated Thrust Bearing," *Proc. of 7th Int. Gas Bearing Symp.*, Cambridge, England, Paper E1.